TSAI'S MODULUS AND DOUBLE-DOUBLE LAMINATES IN THE DESIGN OF ADVANCED COMPOSITE STRUCTURES

Scott L.J. Millen [1], M. A. Aravand [1], Zahur Ullah [1] and Brian G. Falzon [1,2]

[1] Advanced Composites Research Group (ACRG), School of Mechanical and Aerospace Engineering, Queen's University Belfast, Belfast, Northern Ireland (scott.millen@qub.ac.uk, m.aravand@qub.ac.uk, z.ullah@qub.ac.uk)
[2] School of Engineering, STEM College, RMIT University, Melbourne, VIC, 3001, Australia (brian.falzon@rmit.edu.au)

Keywords: Impact behaviour, Finite element analysis (FEA), Tsai's Modulus, Double-Double, Elastic Properties

ABSTRACT

Alternative 'Double-Double' (DD) laminates have been proposed to replace legacy quad laminates (LQL), i.e. conventional laminates, due to potential advantageous design properties that such layups provide. However, limited analysis has been undertaken on these new laminates. This work presents comparative high fidelity computational finite element (FE) modelling of low-velocity impact (LVI) damage and compression-after-impact (CAI) strength of both 'Legacy Quad Laminates' (LQL) and 'Double-Double' DD laminates, using a validated FE modelling approach. An in-house intralaminar damage model and an established interlaminar cohesive model are used. Results show that DD laminates are effective replacements for UD LQL under both LVI and CAI loading conditions. It is shown that delamination damage may be reduced with DDs. Potential weight savings can be achieved with the use of DD laminates as well as simplifying manufacturing processes. In the cases presented herein, CAI residual strength increased with the use of a DD laminate over a traditional LQL.

1 INTRODUCTION

Trace, more recently referred to as Tsai's Modulus [1], an invariant material property derived from the plane stress stiffness matrix, Eq. 1, can be used to help with preliminary design.

$$Tr(Q) = Q_{11}+Q_{22}+2Q_{66} \tag{1}$$

Invariants are not affected by ply orientation and an analytical method such as Tsai's Modulus can create a significant reduction in the number of experimental tests required to generate acceptable material data for preliminary design or screening on the basis of elastic properties [2]. This is especially true where a building block approach in structural design is used, as is typical in the Aerospace industry. With Tsai's Modulus it is possible to predict laminate elastic properties and normalised in-plane, coupling and flexural laminate stiffness matrices by providing only E_1 and ν_{12} of the constituent lamina [2].

Legacy laminates made from strict combinations of 0°, 45° and 90° plies, have many design rules imposed on them, such as mid-plane symmetry. So called double-double (DD) laminates have been proposed by Tsai et al. [3] and can replace traditional legacy laminates. DD laminates require only two angles, [±φ/±Ψ], creating a four ply sub-laminate using any angles. It is argued that for every required orthotropic stiffness, a number of layups would be satisfactory. This would lead to a simplification in terms of manufacturing and repair.

Several advantages of the double-double laminate have been stated by Tsai et al. [3]; DD laminates are lighter and have higher strength than legacy layups, they are naturally symmetric due to their large number of repeating sub-laminates and ply drop can be done one ply at a time rather than two at a time for legacy layups.

To-date, high fidelity computational modelling of DD laminates has been limited. Vermes et al. [4,5] used a combination of Lam search and finite element method (FEM) tools. The authors demonstrated that the use of Tsai's modulus and DD laminates led to significant weight savings compared to LQLs in standard and open-hole tension and compression specimens. To-date only a single reference has compared the low-velocity impact (LVI) response of a DD laminate and a LQL of equivalent stiffness and thickness [6]. However, this study compared only the standard paired DD sub-laminate [±φ/±Ψ] with a LQL. Recently, Tsai [7] noted that the standard paired DD sub-laminate [±φ/±Ψ] can make homogenisation more difficult in some cases. Therefore, Tsai proposed that the [±φ/±Ψ] sub-laminate building block can be modified to three staggered sub-laminates [φ/-Ψ/-φ/Ψ], [φ/Ψ/-φ/-Ψ] or [φ/-Ψ/Ψ/-φ].

No direct comparison has been presented in literature for LQLs and DDs for the same material properties. However, the use of high-fidelity modelling and CAI analysis can provide the specimen strength without the need to plot failure envelopes. DD laminates are of growing interest to the research community and industry alike. Thorough analysis and comparison between DD laminates and LQLs is still nascent. Therefore, this work presents DD laminate replacements for a LQL. LVI/CAI simulations are subsequently conducted to compare the performance of DD and LQ laminates in terms of LVI damage predictions and CAI residual strength.

2 METHODOLOGY

2.1 Intralaminar Damage Model

An in-house intralaminar damage model was used in this work. This damage model can capture both fibre-dominated damage (through a quadratic strain-based failure criterion) and matrix-dominated damage (through a failure criterion modified and adapted by Catalanotti et al. [8]), and permits load reversal. It has an advanced characterstic length calculation using an approach proposed by Chiu et al. [9] based on a search algorithm which maximises damage inititation functions. A non-linear shear model with kinematic hardening [10], and robust element deletion control. This intralaminar damage model has been used extensively for LVI/CAI modelling and composite crushing and more details about the theoretical foundations of the model and validation can be found in refs. [11–15].

2.2 LVI/CAI simulations

The FE models used to simulate LVI/CAI measured 150 x 100 mm and were placed on a picture frame support leaving an unsupported region of 125 mm x 75 mm, following the Airbus Industries Test Method (AITM 1-0010 [16]). The impactor was modelled as a spherically shaped, analytical rigid solid. The general model and boundary conditions for both LVI and CAI are shown in Figure 1. Specimens were meshed using C3D8R elements and the mesh was refined in a region around the impact zone. All simulations were executed using ABAQUS/Explicit.

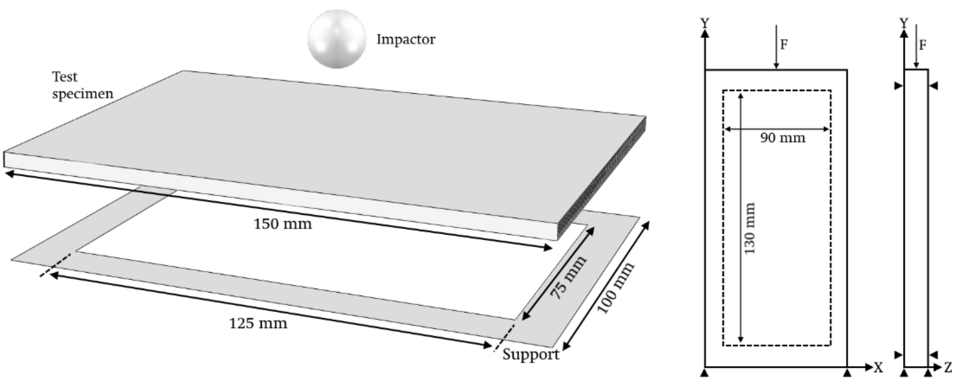

Figure 1: Impact (left) and CAI (right) simulation geometry and boundary conditions.

2.3 Test Specimen

The test specimen considered in this work was taken from literature [11]. This specimen had a LQL stacking sequence of $[0_2/45_2/90_2/\text{-}45_2]_s$, i.e. the percentage of (0°/±45°/90°) being (25/50/25), and was manufactured from T700GC/M21, properties shown in Table 1, with a ply thickness of 0.26 mm. Impact conditions matched the relevant experiments. Therefore, the impact energy was 25J and the impactor had a diameter of 16 mm and mass of 2 kg. After impact, boundary conditions were updated for CAI simulation, shown in Figure 1.

Table 1: Material properties for numerical simulations

Ply properties	
T700GC/M21	E_{11}=130 GPa; E_{22}=7.70 GPa; G_{12}=4.8 GPa; $\nu_{12} = \nu_{13} = 0.33$; X_T=2080 MPa; X_C=1250 MPa; Y_T=60 MPa; Y_C=290 MPa; S_{12}= 110 MPa
Interface properties	k_N = 120 GPa/mm; $k_S = k_T$ = 120 GPa/mm; N = 20 MPa; S = T = 36 MPa; G_{IC} = 600 J/m^2; $G_{IIC} = G_{IIIC}$ = 2100 J/m^2

2.4 Initial model validation

Prior to the comparison of DD impact simulation results with those for the LQL, the LQL model was validated against the available experimental data. Results of this validation are shown in Figure 2 where impact and CAI predictions from the simulations are plotted against the experimental data. Excellent agreement was obtained between the experiments and simulations for impact force-time curves while the predicted CAI strength was within 5% of the relevant experiment.

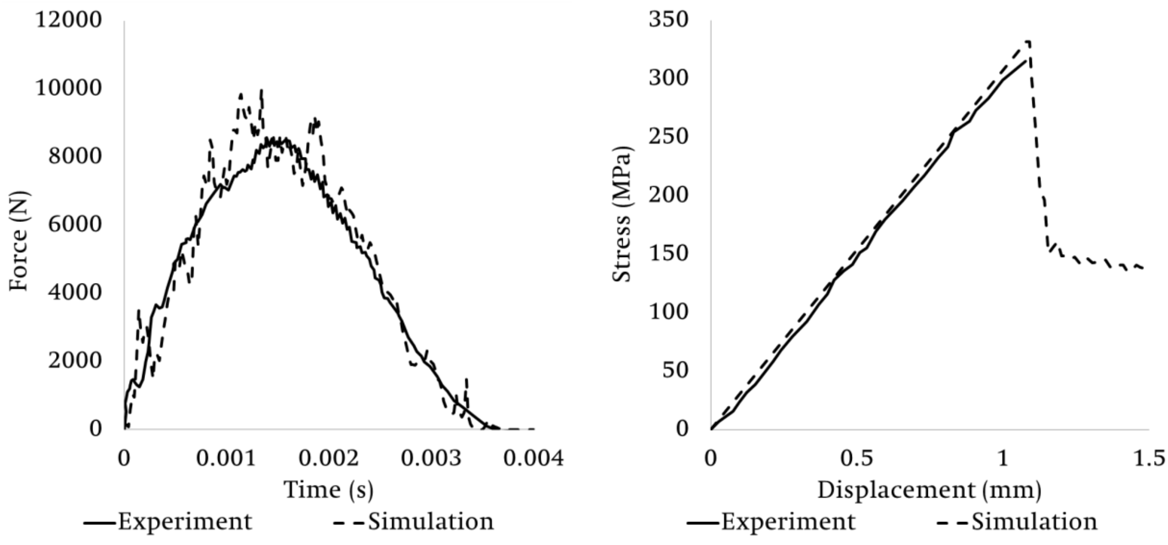

a) Force-time plot

b) CAI residual strength plot

Figure 2: Validation of simulations using LQLs and experimental data

2.5 Double-Double (DD) laminate generation

A combination of *Lam search* [5,17] and the simplified design tool generated in refs. [18,19] were used to find the corresponding DD for the LQL in this study. Based on the extensional stiffness matrix the best DD laminate for the LQL $[0_2/45_2/90_2/-45_2]_s$ was $[\pm22.5/\pm67.5]_{4T}$. Table 1 shows that a perfect match could be achieved with the $[A]^*$ matrix of the LQL. Larger variation occurred for the $[D]^*$ matrix, for example D_{11}^* was 47% lower for the DD laminate.

However, since impact is largely dependent on the bending stiffness of the laminate, this DD was optimised to match the bending stiffness of the LQL and the resulting DD sub-laminate building block was [±9.5/±39.5]. In both $[\pm22/\pm67]_{4T}$ and $[\pm9.5/\pm39.5]_{4T}$ DDs, membrane coupling occurred, and therefore, these laminates could not be considered fully homogenized, Table 2. Therefore, the staggered DD laminate layups proposed by Tsai [7] were studied. **Error! Reference source not found.**he "staggered 3" DD laminate, $[9.5/-39.5/39.5/-9.5]_{4T}$ in this case, was able to achieve a value of D_{11}^*which was 1.6% larger than the LQL but eliminated membrane coupling. Therefore, this DD laminate could be considered homogenised and a suitable replacement for the LQL.

Table 2: Specimen layups and $[ABD]^*$values

	LQL	Paired DD $[\pm\varphi/\pm\Psi]_{rT}$	Paired DD $[\pm\varphi/\pm\Psi]_{rT}$	Staggered 3 DD $[\varphi/-\Psi/\Psi/-\varphi]_{rT}$
(GPa)	(25/50/25)	$[\pm22/\pm67]_{4T}$	$[\pm9.5/\pm39.5]_{4T}$	$[9.5/-39.5/39.5/-9.5]_{4T}$
A_{11}^*	56.5	55.8	89.0	89.0
A_{22}^*	56.5	54.3	19.0	19.0
A_{66}^*	20.5	19.1	20.1	20.1
A_{12}^*	17.0	16.8	17.8	17.8
$\lvert B_{11}^*\rvert$	0.0	5.5	4.4	0.0
$\lvert B_{22}^*\rvert$	0.0	5.4	1.4	0.0
$\lvert B_{66}^*\rvert$	0.0	0.1	1.5	0.0
$\lvert B_{12}^*\rvert$	0.0	0.1	1.5	0.0
D_{11}^*	90.1	55.8	89.0	90.6
D_{22}^*	32.4	54.3	19.0	18.5
D_{66}^*	15.7	19.1	20.1	19.5
D_{12}^*	10.6	16.8	17.8	17.3

Therefore, the following laminates would be compared LQL: $[0_2/45_2/90_2/-45_2]_s$, DD: $[\pm22.5/\pm67.5]_{4T}$, $[9.5/-39.5/39.5/-9.5]_{4T}$.

DD also presents the possibility of using thinner laminates than LQLs. Therefore, simulations started with a DD laminate equal to the thickness of the equivalent LQL. Simulations were then repeated, removing one DD sub-laminate at a time and comparing the damage predictions until perforation. The best alternative DD laminate was then identified, assumed to be the thinnest specimen with the largest residual CAI strength, indicating the structural integrity of the specimen.

3 RESULTS

Initially, results for the LQL, paired DD laminate found using A_{11}^*, $[\pm22/\pm67]_{4T}$, and the homogenised DD $[9.5/-39.5/39.5/-9.5]_{4T}$ are presented in Figure 3. Results show that the peak force for the extensional stiffness-based specimen $[\pm22/\pm67]_{4T}$ was 14% higher than the LQL. The peak force of the homogenised DD was 7% higher than the LQL.

Comparing CAI results, the residual strength of the LQL was 198 MPa. However, for the extensional stiffness-based specimen $[\pm22/\pm67]_{4T}$, this increased by 17% to 232 MPa. Optimising for the $[D]^*$ matrix and homogenisation increased this further to 306 MPa.

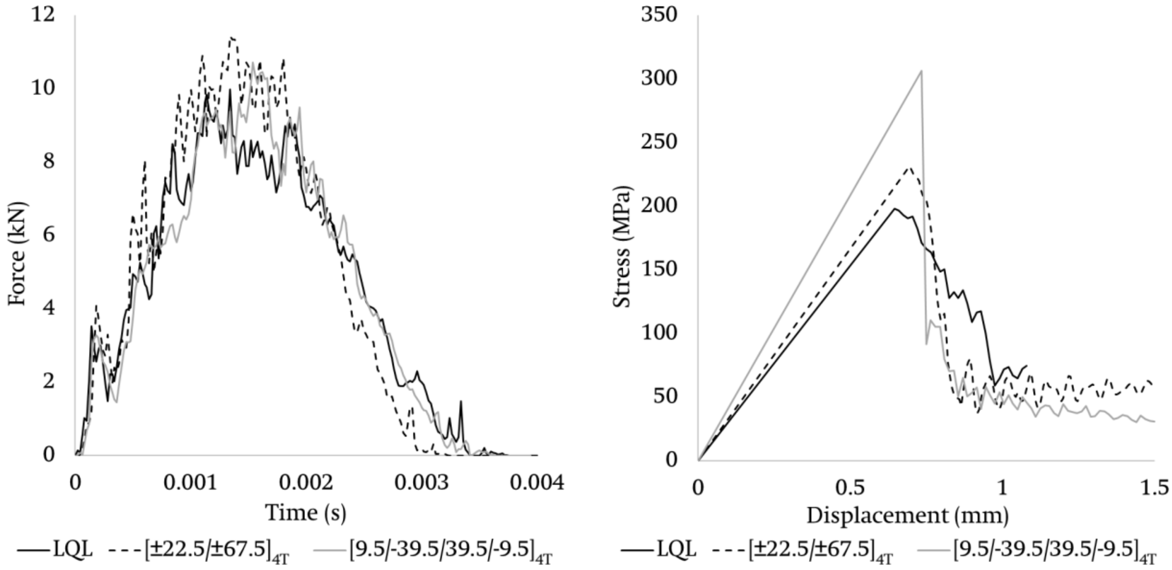

a) Force-time plot

b) CAI residual strength plot

Figure 3: Impact and CAI results for LQL, paired DD based on A_{11}^*, and homogenised DD

Figure 4 shows the superimposed interlaminar delamination plots after impact for each specimen. It can be seen that delamination damage predictions after impact for both DD laminates were more focussed around the centre of the specimen and the total delamination area reduced in each case.

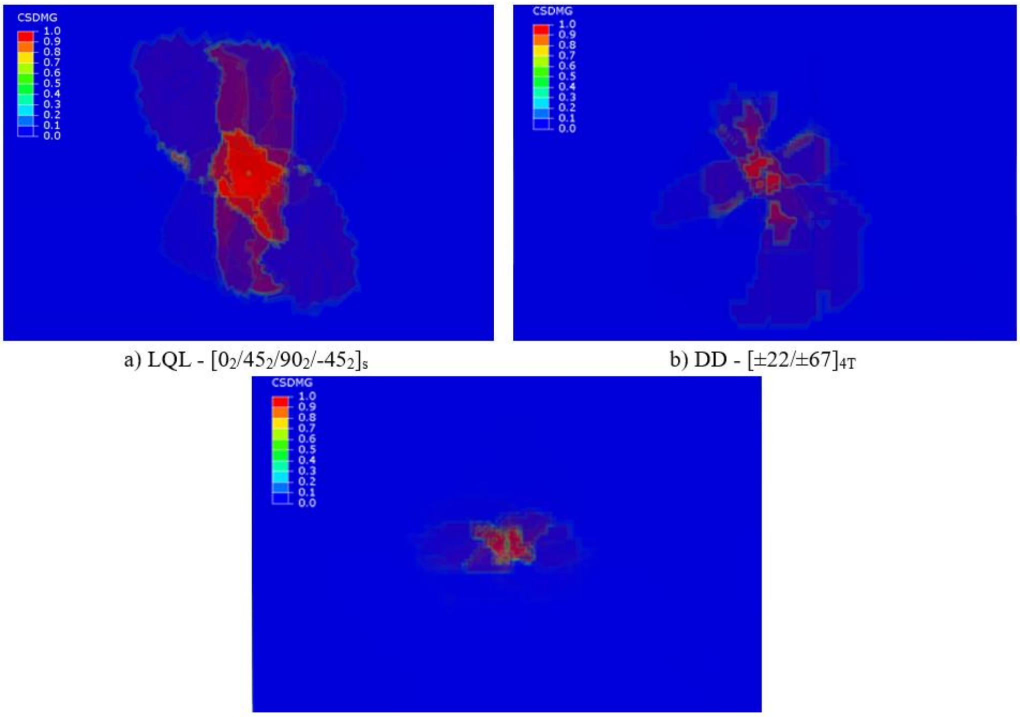

a) LQL - $[0_2/45_2/90_2/-45_2]_s$

b) DD - $[\pm22/\pm67]_{4T}$

c) DD - $[9.5/-39.5/39.5/-9.5]_{4T}$

Figure 4: Comparison of predicted impact delamination for each specimen

3.1 Comparison of DD results when removing sub-laminates

Focusing on the DD laminate results for the homogenised specimen optimised to match the bending stiffness of the LQL, ([9.5/-39.5/39.5/-9.5]rT), these can illustrate the effect of sub-laminate removal on damage tolerance.

Initially, a DD laminate of the same thickness produced a higher peak force, +7 %, Figure 5, when compared with the LQL. Removing one [9.5/-39.5/39.5/-9.5] sub-laminate produced a lower peak force than the first DD, but with a 32% increase in peak displacement over the experiment. Removing a second sub-laminate resulted in complete failure of the specimen under an impact load of 25J. Figure 6 shows the predicted delamination damage. Figure 6a and Figure 6c show that even with the removal of one or two sub-laminates, the DD specimen could still provide adequate resistance to LVI.

Comparing CAI predictions of the $[9.5/-39.5/39.5/-9.5]_{4T}$ 4.16 mm thick DD with the thinner 3.12 mm thick DD $[9.5/-39.5/39.5/-9.5]_{3T}$ the residual strength for the damaged 3.12 mm thick DD was 321 MPa, 62% higher than the damaged LQL and 5% higher than the 4.16 mm thick DD laminate.

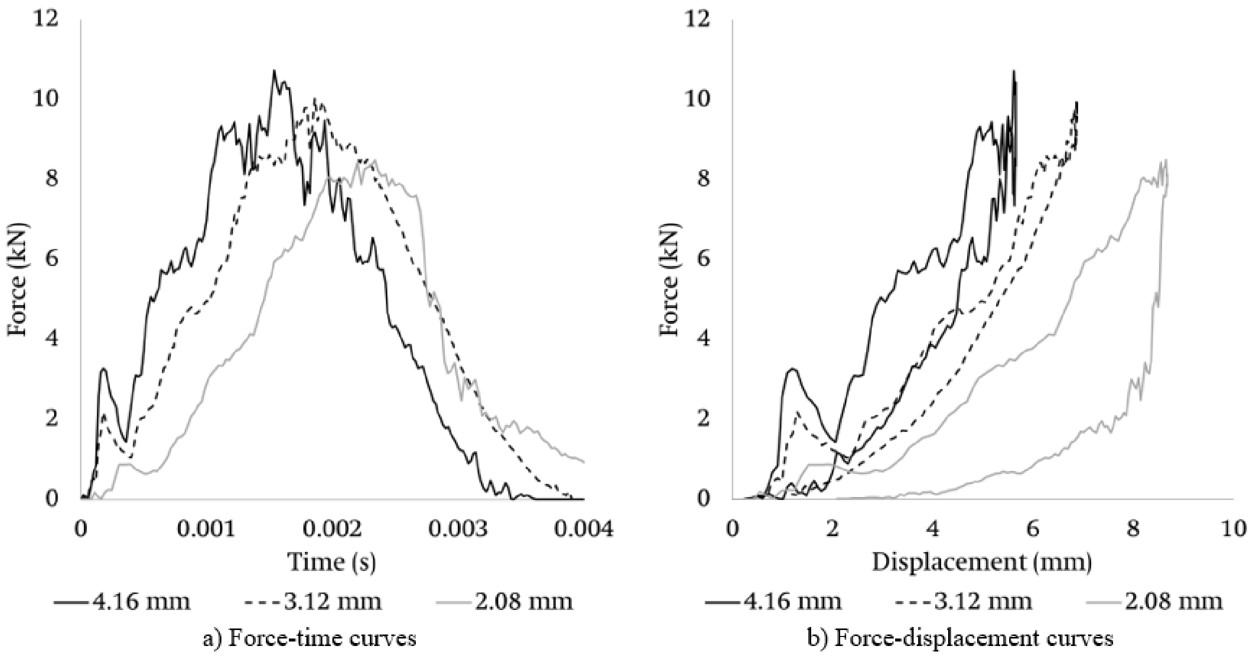

Figure 5: Force-time/force-displacement plots showing the effect of the removal of one sub-laminate at a time for $[9.5/-39.5/39.5/-9.5]_{rT}$.

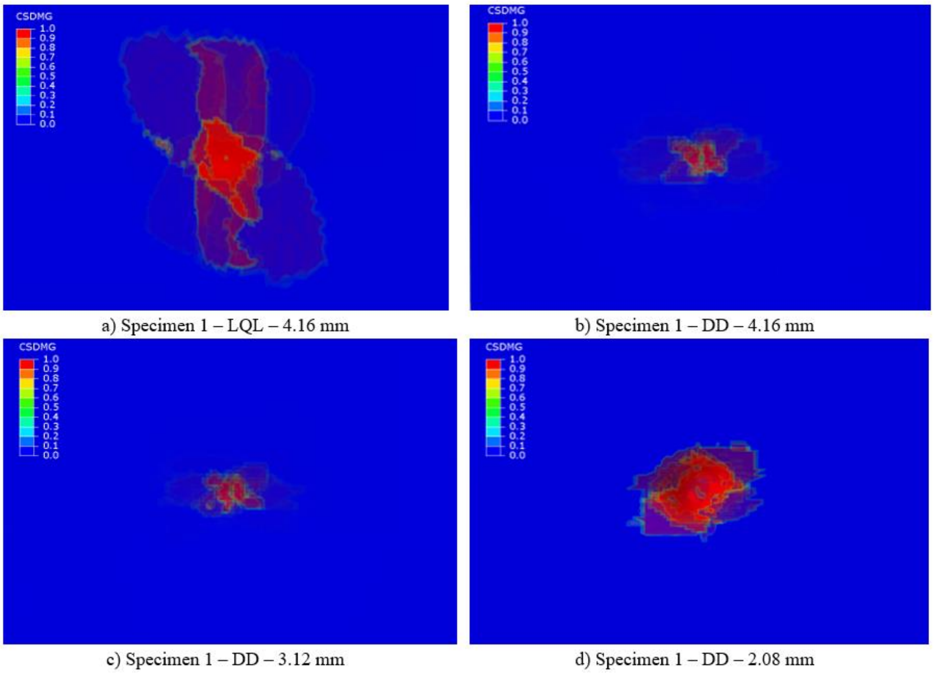

Figure 6: Effect of the removal of one sub-laminate at a time on delamination predictions for [9.5/-39.5/39.5/-9.5]rT

4 CONCLUSIONS

Double-double (DD) laminates have been shown to be capable of replacing legacy quad laminates (LQLs) effectively under both LVI and CAI loading conditions. Choosing a DD sub-laminate to closely match the normalised bending stiffness matrix, $[D]^*$ of the LQL produced significant improvements in laminate performance. However, careful consideration of the effects of membrane-coupling are required. It has been shown that delamination damage can be maintained or reduced when comparing DD and LQLs under LVI. Under CAI, the residual strength of the DD was close to or larger than the LQL for the cases studied herein.

It was also found that a thinner DD laminate could achieve comparable or improved results over the LQL. For example, using the typical approach to select a DD sub-laminate using extensional stiffness matrix matching, CAI residual strength increased by 16% with a 25% reduction in specimen mass. However, for a design focussed on bending stiffness matching and homogenisation, CAI residual strength increased by up to 62%.

While this work has focussed on computational modelling, future work aims to further support these findings through an LVI/CAI experimental programme to compare legacy and DD layups and further validate the simulations in this work.

ACKNOWLEDGEMENTS

This study was conducted within the Belfast Maritime Consortium UKRI Strength in Places project, ‘Decarbonisation of Maritime Transportation: A return to Commercial Sailing’ led by Artemis Technologies, Project no. 107138. Significant contribution and knowledge transfer from Professor Stephen W. Tsai and the team at Stanford University is also gratefully acknowledged. Support and assistance by PhD student Aidan Hawkins is also acknowledged.

REFERENCES

[1] Arteiro A, Sharma N, Melo JDD, Ha SK, Miravete A, Miyano Y, et al. A case for Tsai's Modulus, an invariant-based approach to stiffness. Compos Struct 2020;252:112683. https://doi.org/10.1016/j.compstruct.2020.112683.

[2] Millen SLJ, Falzon BG, Aravand MA. Invariant Based Approaches in the Design of Composite Laminates. Composites Science and Technology 2020.

[3] Tsai SW, Sharma N, Arteiro A, Roy S, Rainsberger B. Composite double-double and grid/skin structures. 1st ed. Composites Design Group, Aeronautics & Astronautics Department, Stanford University; 2019.

[4] Vermes B, Tsai SW, Riccio A, Di Caprio F, Roy S. Application of the Tsai's modulus and double-double concepts to the definition of a new affordable design approach for composite laminates. Compos Struct 2020:113246. https://doi.org/10.1016/j.compstruct.2020.113246.

[5] Vermes B, Tsai SW, Massard T, Springer GS, Czigany T. Design of laminates by a novel '"double-double'''' layup."' Thin-Walled Structures 2021;165. https://doi.org/10.1016/j.tws.2021.107954.

[6] Dantas R, Targino TG, Cardoso C, Paiva E, Carlos R, Freire S, et al. Low velocity impact response of non-traditional double-double laminates. J Compos Mater 2023. https://doi.org/10.1177/00219983231163513.

[7] Tsai SW. Double–double: New family of composite laminates. AIAA Journal 2021;59:4293–305. https://doi.org/10.2514/1.J060659.

[8] Catalanotti G, Camanho PP, Marques AT. Three-dimensional failure criteria for fiber-reinforced laminates. Compos Struct 2013;95:63–79. https://doi.org/10.1016/j.compstruct.2012.07.016.

[9] Chiu LNS, Falzon BG, Boman R. A continuum damage mechanics model for the analysis of the crashworthiness of composite structures: a work in progress. Proceedings of the 15th Australian Aeronautical Conference, Melbourne, Australia: 2013.

[10] Tan W, Falzon BG. Modelling the nonlinear behaviour and fracture process of AS4/PEKK thermoplastic composite under shear loading. Compos Sci Technol 2016;126:60–77. https://doi.org/10.1016/j.compscitech.2016.02.008.

[11] Tan W, Falzon BG, Chiu LNS, Price M. Predicting low velocity impact damage and Compression-After-Impact (CAI) behaviour of composite laminates. Compos Part A Appl Sci Manuf 2015;71:212–26. https://doi.org/10.1016/j.compositesa.2015.01.025.

[12] Faggiani A, Falzon BG. Predicting low-velocity impact damage on a stiffened composite panel. Compos Part A Appl Sci Manuf 2010;41:737–49. https://doi.org/10.1016/j.compositesa.2010.02.005.

[13] Falzon BG, Apruzzese P. Numerical analysis of intralaminar failure mechanisms in composite structures. Part I: FE implementation. Compos Struct 2011;93:1039–46. https://doi.org/10.1016/j.compstruct.2010.06.028.

[14] Tan W, Falzon BG. Modelling the crush behaviour of thermoplastic composites. Compos Sci Technol 2016;134:57–71. https://doi.org/10.1016/j.compscitech.2016.07.015.

[15] Tan W, Falzon BG, Price M. Predicting the crushing behaviour of composite material using high-fidelity finite element modelling. International Journal of Crashworthiness 2015;20:60–77. https://doi.org/10.1080/13588265.2014.972122.

[16] AITM Airbus Test Method. Fiber Reinforced plastics determination of compression strength after impact. 2010.

[17] Tsai SW, Sharma N, Arteiro A, Roy S, Rainsberger B. Composite double-double and grid/skin structures. 1st ed. Composites Design Group, Aeronautics & Astronautics Department, Stanford University; 2019.

[18] Millen SLJ, Aravand MA. Assessing the relative conservatism of the unit circle failure envelope. Composites Communications 2021;24. https://doi.org/10.1016/j.coco.2021.100690.

[19] Millen SLJ, Falzon BG, Aravand MA. Invariant Based Approaches in the Design of Composite Laminates. Compos Sci Technol 2021;202. https://doi.org/10.1016/j.compscitech.2020.108526.